© 2016. Published by The Company of Biologists Ltd | Journal of Experimental Biology (2016) 219, 168-174 doi:10.1242/jeb.124594

REVIEW

Myosin isoforms and the mechanochemical cross-bridge cycle

Jonathan Walklate*, Zoltan Ujfalusi* and Michael A. Geeves‡

ABSTRACT

At the latest count the myosin family includes 35 distinct groups, all of which have the conserved myosin motor domain attached to a neck or lever arm, followed by a highly variable tail or cargo binding region. The motor domain has an ATPase activity that is activated by the presence of actin. One feature of the myosin ATPase cycle is that it involves an association/dissociation with actin for each ATP hydrolysed. The cycle has been described in detail for a large number of myosins from different classes. In each case the cycle is similar, but the balance between the different molecular events in the cycle has been altered to produce a range of very different mechanical activities. Myosin may spend most of the ATPase cycle attached to actin (high duty ratio), as in the processive myosin (e.g. myosin V) or the strain-sensing myosins (e.g. myosin 1c). In contrast, most muscle myosins spend 80% of their ATPase cycle detached from actin. Within the myosin IIs found in human muscle, there are 11 different sarcomeric myosin isoforms, two smooth muscle isoforms as well as three non-muscle isoforms. We have been exploring how the different myosin isoforms have adapted the cross-bridge cycle to generate different types of mechanical activity and how this goes wrong in inherited myopathies. The ideas are outlined here.

KEY WORDS: Muscle, Contraction, Human, Cardiac, Skeletal

Introduction

Myosins are a large family of ATP-driven mechanoenzymes that generate a wide range of mechanical activities using the actin cytoskeleton as a track to move along like a locomotive (Krendel and Mooseker, 2005). Genomic studies have revealed up to 35 classes of myosin, each with a highly conserved motor domain consisting of ~800 amino acids and a variable tail referred to as the cargo binding domain (Odronitz and Kollmar, 2007). Despite the variability in the tail domain sequence, analysis suggests that the motor and cargo binding domains have coevolved to match each cargo with the specific type of motor activity required for each motor function (Krendel and Mooseker, 2005; Weiss and Leinwand, 1996).

Structural studies coupled with biochemical kinetics have revealed details of the ATPase cycle that drives mechanical activity (see Fig. 1 and for reviews, see De La Cruz and Ostap, 2004; Geeves and Holmes, 1999, 2005; Sweeney and Houdusse, 2010). The conserved motor domain contains an actin binding site(s) that is split by a major cleft in the motor domain, and tight binding of actin requires the cleft to be closed. ATP binding opens the cleft and thereby dissociates actin from myosin. Hydrolysis of ATP in its binding pocket is required to 'prime' the myosin before actin can rebind, close the cleft and displace the hydrolysis products, first phosphate (P_i) followed by ADP. During the displacement of products the motor goes through what is referred to as the power stroke or working stroke, in which small movements around the nucleotide pocket are amplified via a lever arm to generate a few piconewtons of force or a few nanometers of movement of the 'cargo' relative to the actin binding site. A recovery or repriming stroke linked to the ATP hydrolysis step is required while the motor is detached from actin to complete the cycle.

Studies of myosin motor domain have revealed high-resolution structures of many of the intermediates around the cycle. Biochemical kinetic studies have defined the rate and equilibrium constants for each of the steps in the cycle. Every myosin that has been studied has the same sequence of events in the cycle (Fig. 1). Differences between myosin classes are due to alterations in the length and shape of the lever arm (altering the size and direction of the movement) and variations in the rates and equilibrium constants of the events in the cycle. The whole cycle can proceed at very different overall velocities and with variations in the fraction of cycle time the motor spends in each state. Of particular significance are changes in the duty ratio, the fraction of time in each ATPase cycle that the motor spends tightly attached to actin. Low duty ratio myosin can spend 10% or less of each ATP hydrolysis cycle tightly attached to actin. In this case, effective transport of cargo requires cooperation between several motors working together. In such motors, the myosin with ADP and phosphate tightly bound in the active site (MDPi, see Fig. 1) is a stable complex that is primed to contribute to transport, but is stable until it can find an appropriate actin site to bind to. In contrast, processive motors such as myosin V spend most of their ATPase cycle tightly bound to actin. For the dimeric myosin V, the myosin head with ADP tightly bound remains tightly bound to actin, and a pull from the leading partner head signals the rear head to release ADP, leading to the ATP-induced detachment of the rear head. This signalling between the two heads allows hand-over-hand walking along an actin filament (Trybus, 2008; Veigel et al., 2005).

Understanding how each myosin is adapted for its specific role requires the contribution of each step in the cycle to be defined, i.e. how the biochemical events at the actin and nucleotide sites are coordinated, how the local structural changes are amplified to produce nanometer scale movements and piconewton forces, and how the mechanical, structural and biochemical changes are coupled for efficient energy transduction.

The central role of ADP in mechanical activity

We recently proposed that the mechanical/motor activity of myosin motors can be classified into four types: fast, powerful movers; slow, efficient force holders; sensors; and processive/signal transducers (Bloemink and Geeves, 2011). In addition to changes in duty ratio across the series, one of the distinguishing features of different types of motor activity is how the ADP release step is used in different ways. As shown in Fig. 2, the loss of Pi to form AMD is the step that generates a mechanical force between actin and myosin, and if the force is great enough, then the two move relative to each other. For efficient use of the mechanical force generated, the lifetime of the attached AMD must be long enough to allow the movement of the cargo to take place and the force to go towards zero. A load-dependent ADP release step – the ADP release is slow

School of Biosciences, University of Kent, Canterbury CT2 7NJ, UK.
*These authors contributed equally to this work

‡Author for correspondence (m.a.geeves@kent.ac.uk)

Journal of Experimental Biology

Journal of Experimental Biology (2016) 219, 168-174 doi:10.1242/jeb.124594

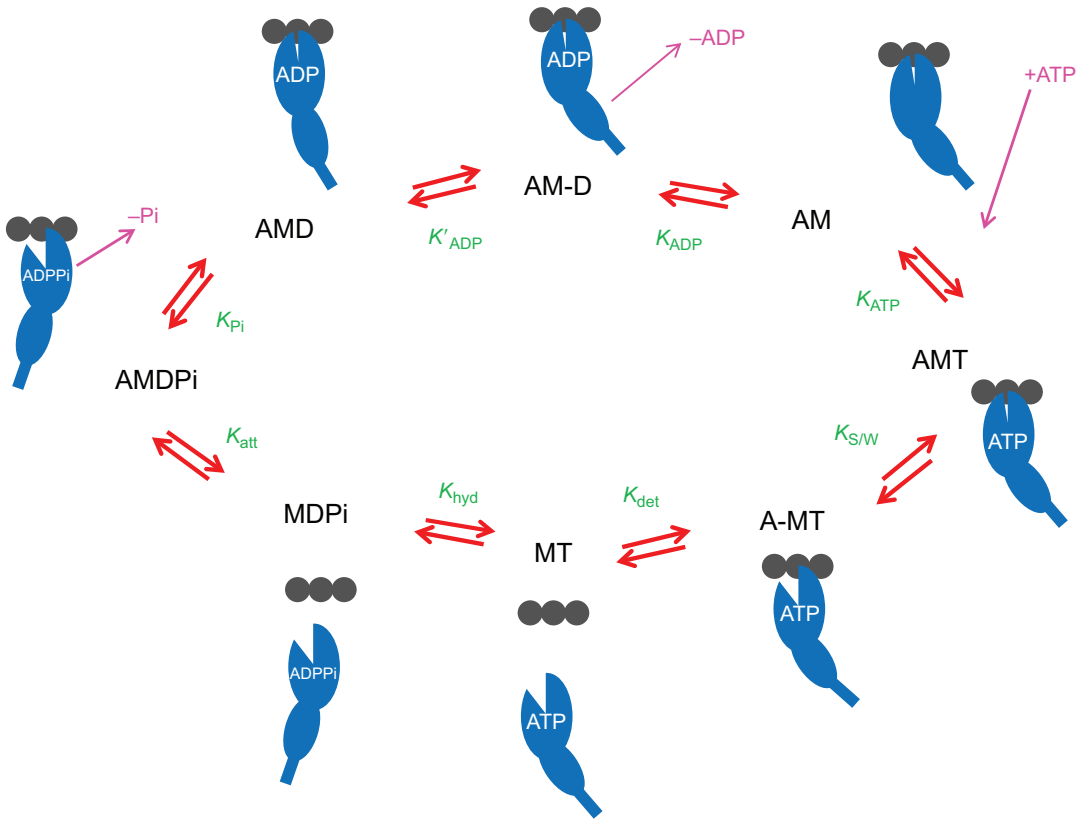

Fig. 1. A minimal ATPase cycle for the actin and myosin cross-bridge cycle. Filled circles represent the actin monomers in a thin filament and the blue shape represents the motor domain of myosin. M is myosin, A is actin, T is ATP, D is ADP and Pi is inorganic phosphate. AMD, for example, represents a complex between actin, myosin and ADP. A hyphen between two letters indicates the association is relatively weak, i.e. AMD represents ADP tightly bound to AM, AM-D represents ADP weakly bound to AM. When detached, or only weakly bound to actin, a large cleft in the 50 kDa domain of the myosin motor is open. Tight binding of myosin binding to actin requires the cleft to close, such that both sides of the cleft contribute to actin binding. The rear of the motor domain (comprising the converter and lever arm) swings through an angle of 60 deg relative to the 50 kDa domain in response to events in the nucleotide pocket. The equilibrium constants for each step are shown in green and are defined as $K_i=k_{+i}/k_{-i}$, where i is the name of the step, k_{+i} is the rate constant in the forward direction and k_{-i} in the reverse direction. Starting with the actin.myosin rigor-like complex, AM, at the top right, ATP binding to AM (K_{ATP}) is followed by a rapid change in myosin conformation, leading to the cleft opening ($K_{S/W}$) and rapid detachment of actin (K_{det}). The opening of the 50 kDa cleft leads to a conformation change in the head that swings the lever-arm/converter domain through 60 deg (the recovery stroke) and positions catalytic residues to hydrolyse ATP (K_{hyd}). After hydrolysis, the myosin can reattach to actin (K_{att}) and the cleft can close; the power stroke and Pi release follow (K_{Pi}). ADP remains firmly attached to myosin until the working stroke is complete, which then allows a conformational change (K'_{ADP}) that then allows ADP to escape, and the cycle is complete (K_{ADP}).

while the load remains on the myosin motor – would ensure that the myosin does not detach until the working stroke (moving the cargo) is complete. Once the force has dissipated, then the ADP can be rapidly released and the cycle continues by the binding of ATP and detachment of the motor from actin. Substantial evidence from high-resolution electron microscopy images and single molecule force measurements have shown that load-dependent structural changes coupled to ADP release are common to many myosins (Greenberg et al., 2012; Kovács et al., 2007; Veigel et al., 2003, 2005). Such a mechanism is shown in Fig. 2.

In Fig. 2A, Pi release is coupled to a swing of the myosin lever arm that can generate a mechanical force indicated by the elastic element, shown for convenience in the connector between the motor and the cargo. Before ADP release can occur, the motor domain must go through a second conformational change that swings the lever arm further in the same direction as the power stroke. If there is a load on the motor, this additional movement against the load will be greatly inhibited. Different types of motors can be created by varying the free energy (and hence the equilibrium constant) associated with the conformational change and the energy stored in the elastic element available to do external work. As shown in Fig. 2B, $K_{C/O}$ (the equilibrium constant for the conformational change that opens the ADP pocket to allow ADP to be released) varies for different classes of myosin. A large value of $K_{C/O}$ means that the reaction takes place with sufficient free energy change to allow the conformational change even against a significant load (if $K_{C/O}>20$ and because $\Delta G°=-RT\ln K_{C/O}$, where $\Delta G°$ is the standard free energy change for the reaction, R is the gas constant and T is absolute temperature, the free energy change associated with the conformational change is large and negative). This is important for a fast-moving motor where speed and power are the primary roles. A smaller value of $K_{C/O}$ (~1–10; $\Delta G°$~between zero and a small negative value, i.e. $-1RT$) will give a myosin that is sensitive to load but where ADP release is possible against small loads – suitable for a slow-moving motor efficient for both force generation and slow movement, e.g. slow or β cardiac muscle myosin, which has a threefold inhibition of ADP release for a 2–4 pN load (Greenberg et al., 2014). A value of $K_{C/O}$ close to 1 ($\Delta G°$~0) produces a motor very sensitive to load, and complete inhibition of ADP release is possible for modest loads (e.g. myosin 1b/c, a 100-fold inhibition of ADP release for moderate loads; Greenberg et al., 2012), ideal for a strain sensor – it will hold modest loads for long periods of time with low ATP turnover. For a $K_{C/O}<0.1$ ($\Delta G°>+1RT$), the ADP release is inhibited even without load compared with other myosins, and ADP release can be rate limiting for the unloaded

Journal of Experimental Biology (2016) 219, 168-174 doi:10.1242/jeb.124594

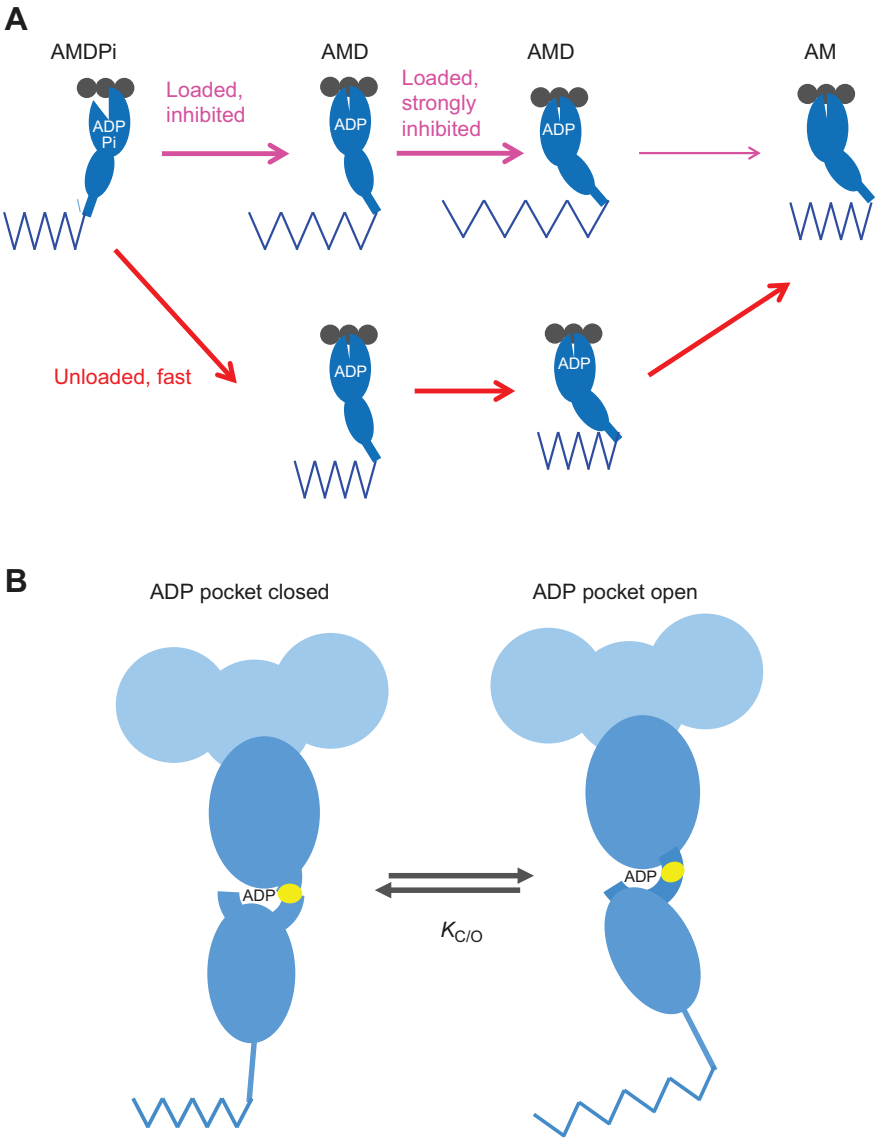

Fig. 2. Load dependence of ADP release. (A) Load will inhibit both the power stroke (generation of force against a load) and the working stroke, as well as the completion of the lever arm swing against load. (B) After Pi release, ADP is held in a pocket that is closed to retain ADP. A further rotation in the direction of the load is required for the pocket to open. If the working stroke (dissipation of energy in the spring) is incomplete because of the load, then the second swing is inhibited. The protein conformational change is labelled $K_{C/O}$, and is an indication of a change from pocket closed to open, to allow ADP release. The free energy change associated with this conformational change indicates how much energy (ΔG) is available to work against the load. Different types of motor have very different values for the equilibrium constant and hence available free energy.

ATPase cycle. In such a case, a load will further inhibit an already slow release, but the release can be accelerated by a forward pull by other motors, as in processive myosin V. Such a motor is also a good signal transducer; it holds onto its ADP unless it gains an additional signal from another source, such as calcium binding to the lower stiffness of the lever arm, for example, or a pull forward by another myosin, as in a hand-over-hand processive motor.

Sarcomeric muscle myosin 2

Striated muscles use different isoforms of the dimeric myosin II subgroup to perform 'external' mechanical work. Most mammals express up to a dozen myosin II isoforms, each from a separate gene (Golomb et al., 2003; Schiaffino and Reggiani, 2011; Weiss and Leinwand, 1996). Nomenclature for the isoforms can be confusing, as the isoforms are known historically by the muscle fibre type or tissue initially associated with the isoform, and more recently by the systematic naming of the gene coding for the protein. Table 1 lists the gene and tissue-derived names for the most common mammalian isoforms. There are three non-muscle isoforms (NM2A to C), which are most closely related to the smooth muscle myosin II isoform and 11 sarcomeric myosin isoforms. The sarcomeric muscle isoforms are the three adult fast muscle forms 2a, 2b and 2x, two developmental isoforms, embryonic and perinatal, a specialist extraocular isoform and the two cardiac forms α and β (β is also known as the slow skeletal muscle isoform). There are three other isoforms found in some species and tissues, commonly referred to using the gene name MYH 15, 16 and 7b. The sarcomeric isoforms all have >80% sequence identity, while the non-muscle and smooth muscle isoforms are only 40% identical to the sarcomeric forms.

One of the interests in myosin structures is how the different myosin isoforms are adapted for the different mechanical roles in different muscle fibre types. The adult skeletal and cardiac muscle types are the best described and the mechanical contraction parameters vary by as much 10-fold between isoforms. Much less has research been done on the embryonic, perinatal and extraocular muscle fibres because it is rare to find a muscle fibre expressing just a single pure form of these isoforms (see Racca et al., 2013). Table 2 lists some of the key contraction parameters defined for the adult human skeletal muscle forms based on the summary in a major review by Bottinelli and Reggiani (2000). A similar set of parameters is available from a study of myofibrils and myosin isolated from cardiac ventricle and atrial tissue, which express predominantly β and α cardiac myosin, respectively (Piroddi et al., 2007).

Journal of Experimental Biology

Journal of Experimental Biology (2016) 219, 168-174 doi:10.1242/jeb.124594

Table 1. Mammalian myosin isoform nomenclature

Tissue-based name (abbreviation)	Myosin heavy chain gene (MYH*)	Notes
Fast skeletal 2d or 2x (2x)	MYH1	
Fast skeletal 2a (2a)	MYH2	
Fast skeletal 2b (2b)	MYH4	Not thought to be expressed in humans
Slow tonic	MYH7b	
Cardiac β/slow skeletal (slow, 1 or β)	MYH6	
Cardiac α (α)	MYH7	α
Perinatal (peri)	MYH8	
Embryonic (emb)	MYH3	
Extraocular (EOC)	MYH13	
Smooth muscle (Sm)	MYH11	Two alternatively spliced forms
Non-muscle A (NM2A)	MYH9	
Non-muscle B (NM2B)	MYH10	
Non-muscle C (NM2C)	MYH14	

Based on Fig. 1 of Schiaffino and Reggiani (2011).
*Gene name is MYH in humans and Myh in rats and mice, with the same numbering for the isoforms. The protein (myosin heavy chain) is sometime referred to as MYH or MyHC, with the same numbering as the gene.
There are additional minor isoforms in some tissues/species, e.g. MYH15 and 16.

The maximum shortening velocity for different muscle types varies by up to 10-fold; these differences in shortening velocity are part of the definition of muscle fibres as fast or slow contracting types. In contrast, isometric tension (tension per cross-sectional area of sarcomere or tension per myosin motor) does not change much between isoforms, which is consistent with single molecule data that suggest that the step size and unitary force are relatively constant for muscle myosin IIs (Bottinelli and Reggiani, 2000). However, the ATPase activity in an isometrically contracting muscle differs more than threefold between the fast and slow types, resulting in the tension cost (ATP used per unit of tension per second) being up to threefold higher for fast-type muscles. The 10-fold differences in velocity lead to big differences in the force–velocity relationship for different fibre types, and hence to sixfold variations in the power output as a function of velocity.

In summary, slow-type muscle fibres can hold the same tension as a fast muscle fibre, but with a lower rate of ATP usage (tension cost). However, this results in a lower maximum power output for slow-type muscles. The slow myosin has therefore been adapted for efficient tension holding and slow contraction velocities, while the fast muscle myosins are adapted for high speed and large power generation. In general, the fastest muscles are also anaerobic and therefore ideal for short bursts of intense power output and very high ATP usage.

Shortening velocity

Because the shortening velocity varies markedly between myosin isoform types, this provides an opportunity to examine how different isoforms are adapted for different roles. The maximum shortening velocity is, at least in principle, one of the simpler parameters to define at the muscle fibre level, and for a pure myosin isoform the velocity of movement can also be measured using the *in vitro* motility assay (Kron and Spudich, 1986). Pellegrino et al. (2003) showed that for a muscle fibre expressing a single myosin heavy chain, the maximum shortening velocity was characteristic of the myosin isoform expressed and the maximum velocity observed for each isoform was slower for the myosin from muscles of larger animals compared with small animals (Fig. 3). The same relationship was also found in a motility assay using the same myosins isolated and purified from tissue. Once again, the velocity was characteristic of the isoform and the same isoform from larger animals gave a slower velocity. Thus the myosin isoform expressed defines the maximum velocity of contraction and this velocity is tuned to the size of the animal, presumably by small sequence changes between isoforms and between species.

Current models of the myosin cross-bridge cycle suggest a simple relationship between the maximum velocity and steps in the attached part of the ATPase cycle. If the working stroke of the cross bridge is d (nm) and the velocity for actin sliding over myosin is V (nm s^{-1}), then the lifetime of the attached cross-bridge (τ) cannot be greater than d/V, i.e. $V=d/\tau$. The cross-bridge must detach rapidly once it has completed

Table 2. Mechanical parameters that change and do not change between muscle fibre types or between muscle myosin isoforms, e.g. fast and slow isoforms 2a and 1

Changes between skeletal 2x and slow/β-cardiac	No change (<2-fold)
Isometric ATPase 3-fold	Isometric force/unitary force
Tension cost (tension/ATP) 3-fold	Unitary step/step size
Max. power 6-fold	Unitary force (step×stiffness)
Max. velocity ~10-fold	Max. efficiency 40%
V_{max} ATPase in solution 10-fold	Duty ratio <0.2

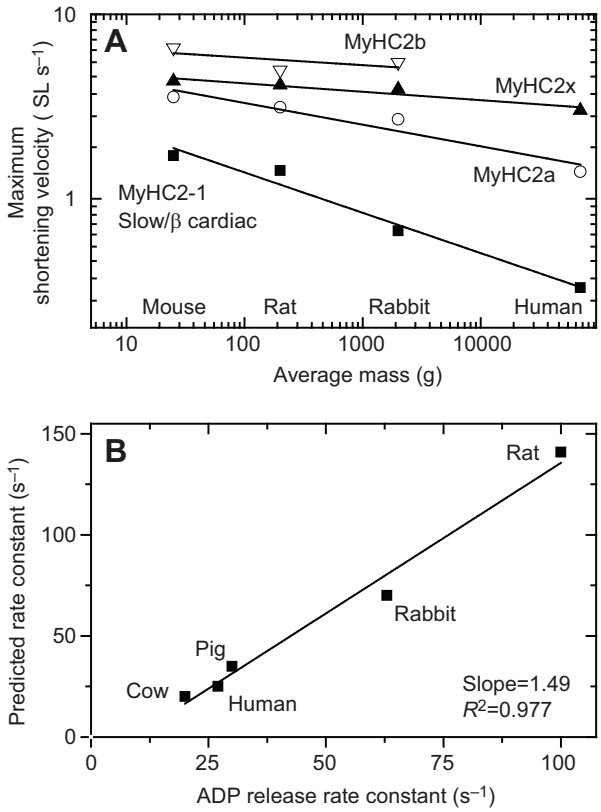

Fig. 3. Relationship between myosin isoform, muscle shortening velocity and the rate constant for ADP release. (A) Maximum shortening velocity of muscle fibres expressing a single myosin isoform, plotted against the average mass of the species the muscle came from. Each isoform has a distinct velocity that is related to the species mass. Data are re-plotted from Pellegrino et al. (2003). (B) Relationship between the measured rate constant for ADP release from the actin.myosin cross-bridge and that predicted from the measured velocity of muscle shortening. Data are shown for slow/β-cardiac myosin. The two parameters show a high correlation with a slope close to 1, which indicates that the rate of ADP release controls velocity. Data are from Deacon et al., 2012 (human) and Bloemink et al., 2007.

Journal of Experimental Biology (2016) 219, 168-174 doi:10.1242/jeb.124594

its working stroke to avoid exerting a drag on the movement. The detachment rate is controlled by the rate at which ATP binds to the cross-bridge and induces cleft opening. For all muscle type myosins measured to date, the ATP-induced dissociation of the cross-bridge is very fast (complete in ~1 ms) and too fast to define the shortening velocity. In contrast, ADP release does vary for different myosin types. Fig. 3B shows the measured rate constant controlling ADP release compared with that predicted from the shortening velocity ($1/\tau$) for a set of slow muscle isoforms (Type 1 or β-cardiac myosin) from different species. This shows a very close fit to the predicted values and suggests that the ADP release does limit the velocity. A factor of two slower, and the ADP release would slow shortening velocity significantly. A factor of two higher, and ADP release would only have a moderate effect on velocity.

For fast muscle isoforms, the measurement of the rate constant of ADP release is not as simple. ADP does not bind tightly enough to form the relevant actin.myosin.ADP complex as shown below, where AMD and AM-D represent an actin.myosin complex with ADP tightly bound (closed pocket) or weakly bound (pocket open) (see Fig. 2B):

$$\mathrm{AMD} \overset{K_{c/o}}{\rightleftharpoons} \mathrm{AM-D} \overset{K_{ADP}}{\rightleftharpoons} \mathrm{AM + D},$$

where $K_{c/o}$ is $\gg 1$ and AMD is not occupied. The ADP release measured is from the AM-D, which is very fast. However, the equilibrium constant of ADP binding (K_{ADP}) can be measured, and does show a close correlation with the velocity of shortening (see Fig. 3). Thus although the ADP release rate constant for fast-type myosins cannot be shown to control shortening, the equilibrium constant does change for myosin isoforms and for different species in a way that does correlate closely with shortening velocity.

Human myosin isoforms

Studies of the different muscle myosin isoforms in humans have been hampered by the availability of preparations of pure myosin. Most muscles contain multiple isoforms and they are not easy to separate. Expression of sarcomeric myosins has been difficult because the folding of the myosins appears to require a complex set of chaperones which remain poorly defined. Recently, Srikakulam and Winkelmann (1999) were able to express distinct myosins in a mouse muscle cell line that naturally has the required folding machinery. The Leinwand group (Deacon et al., 2012; Resnicow et al., 2010) has adapted this method to express the motor domain of human muscle myosins with appropriate purification tags, and eight sarcomeric muscle isoforms have been successfully expressed. The quantities are small (1–2 mg) but useable. Expression of each of the myosin muscle isoforms has allowed us to define the rate and equilibrium constants for most steps round the cycle for each of the human sarcomeric myosin II isoforms; however, equivalent mechanical data are only available for the major adult forms α, β, 2a, 2b and 2x because it is relatively easy to find muscle fibres expressing only one of these isoforms.

We now have a fairly complete analysis of the solution (i.e. unloaded) ATPase cycle for most of the common human muscle isoforms. Analysis of each step around the cycle shows that the steps that change the most are the ATP hydrolysis and the ADP release steps. If these steps change in parallel, then the duty ratio can remain the same but the cycle speed can be different. However, the rate of the Pi release steps is difficult to define unequivocally because it can be difficult to distinguish from a preceding rate-limiting event. Muscle fibre studies of the rates of force development (following a rapid rise in calcium or a period of rapid shortening) give information on events linked to Pi release and are consistent with significant changes in the rate of Pi release for different isoforms. To look at this in more detail, the overall ATPase rates can be used to define the Pi release steps. In the case of human β myosin motor domain, the maximum velocity (V_{max}) and Michaelis–Menten constant (K_m) values have been defined as ~6 s^{-1}, and ~40 μmol l^{-1}, respectively, under our experimental conditions. Using these values, and with known values of the other steps in the cycle, leaves only the Pi release step (K_{Pi}; Fig. 1) and the actin binding constant (K_{att}) unknown. Fitting the ATPase data defines values of K_{att}=75 μmol l^{-1} and k_{+Pi}, the rate constant for Pi release, of 13 s^{-1}. This gives the distribution of the major intermediated in the cycle shown in Fig. 4A. The results are shown for an actin concentration equal to the K_m for actin (i.e. where the velocity of the

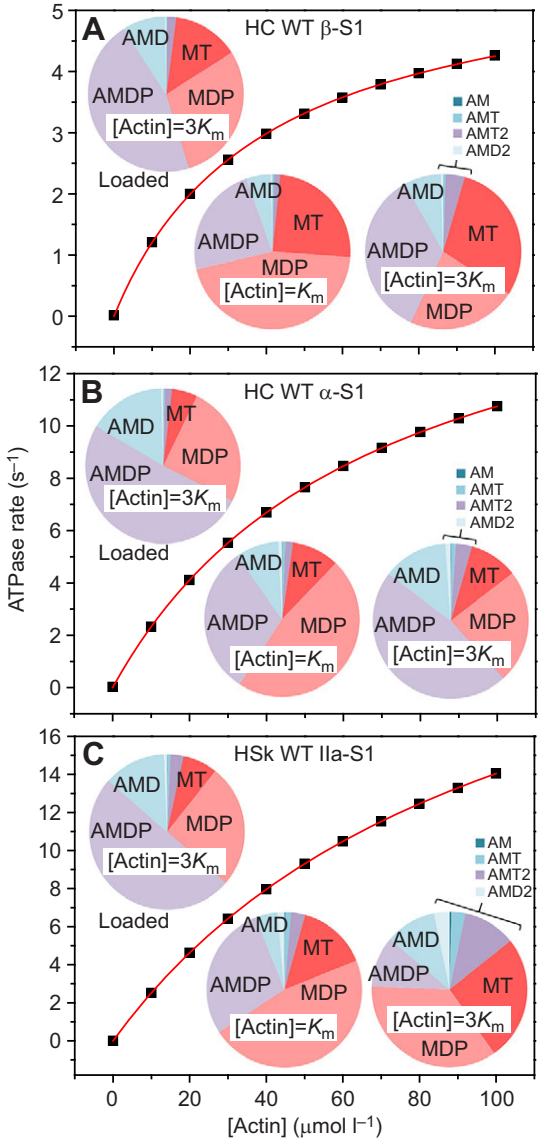

Fig. 4. Dependence of the myosin ATPase on actin concentration and predicted occupancy of each of the states in the ATPase cycle. Predicted ATPase rates for three myosin isoforms and occupancy of the intermediates in the cycle as defined in Fig. 1 under three conditions: at an actin concentration equal to the K_m value, at an actin concentration of 3K_m (v=0.75V_{max}), and at v=0.75V_{max} if the system is loaded such that the rate constants of the Pi release step (k+Pi) and the ADP isomerisation step (K'_{ADP}) are reduced threefold.

Journal of Experimental Biology (2016) 219, 168-174 doi:10.1242/jeb.124594

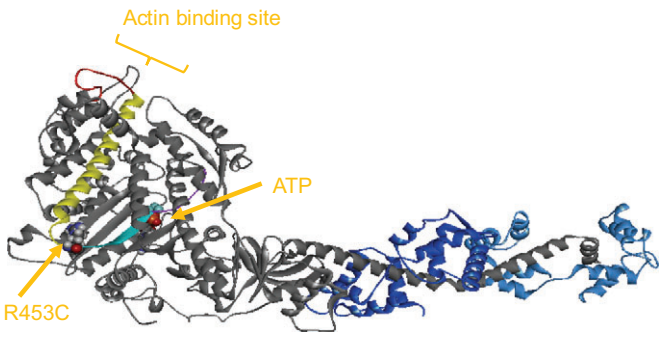

Fig. 5. Location of the R453C mutation in the β-cardiac myosin motor domain. The motor domain is shown in a ribbon diagram format with the R453C side-chain and the ATP shown as space-filling spheres. The main chain is shown in grey and the two light chains in dark blue and light blue. R453 is located on a short surface loop (the HO linker) that connects helix O (yellow) to the fifth strand of the central β-sheet (cyan). The O-helix connects to the actin binding site, while the β-strand is connected to switch 2, part of the ATP binding site. The structure was built from the crystal structure of scallop myosin II (PDB-ID:1KK8) using the human β-myosin sequence and is based on fig. 1 of Bloemink et al. (2014).

reaction v=0.5V_{max}) and when the actin concentration is equal to 3K_m (i.e. v=0.75V_{max}). This indicates the sensitivity of the system to the actin concentration. This is useful for comparison to muscle fibre conditions, as the local concentration of actin for each myosin can vary because of the different geometry of the thick and thin filaments and differing levels of calcium activation.

Taking a similar approach to fast muscle myosin 2a and cardiac α myosin yields the results shown in Fig. 4. Fast muscle myosin 2a has a much faster ATPase (V_{max}) and therefore very much faster ADP and Pi release rates than the β-myosin (Fig. 4B). Those for α cardiac myosin are intermediate between values for β and 2a myosin (Fig. 4C). Despite the differences in the ATPase cycling rates, the fit of the model results in a similar duty ratio for all three myosins.

These are solution conditions; the nearest equivalent in a muscle fibre is under rapid shortening at zero load. In a muscle fibre contracting against a load, the ATPase cycle is inhibited by load, and for a variety of muscles the ATPase rate falls to approximately one-third of its value compared with unloaded conditions (Bottinelli and Reggiani, 2000). If the modelling shown in Fig. 4 is approximately correct in each case, then we can model what is expected for both the Pi and ADP release steps if these are the only steps inhibited by load. A reduction in ADP release has little effect on the ATPase rate unless it is inhibited more than 10-fold while the Pi release rate constant is almost proportional to the V_{max} of the ATPase. If it were only the Pi release step that was inhibited by load, then there would be little change in the proportion of cross-bridges in the strongly attached state. This is inconsistent with the expectation that there will be more force-holding bridges and a slower shortening velocity under isometric conditions. The ADP step is therefore expected to be inhibited, as seen with *in vitro* single molecule studies (Greenberg et al., 2014; Kovács et al., 2007; Veigel et al., 2003). The effect of slowing the ADP step by a factor of three in each case, and slowing the Pi release step (usually fivefold to sixfold) sufficient to slow the ATPase cycle by a factor of three, is shown in Fig. 4 ('loaded'). The plot shows the change in population of the states in the cycle under loaded conditions. In each case, the population of the AMD state increases approximately 30%, i.e. a one-third increase in the number of bridges holding the load.

At the primary structure level we know where the changes in sequence occur between the different isoforms. How they alter the myosin behaviour is not so simple to define. Analysis of myosin motor domain sequences for different myosin isoforms and for the same isoform in different species is one way to attempt to define which sequence changes are responsible for different mechanical activities. An alternative is to look at the role of specific mutations, such as those that occur in myopathies. There are 300 known mutations in the myosin motor domain of β-cardiac myosin associated with heart disease (Colegrave and Peckham, 2014; Moore et al., 2012). Currently, designing mutations in a sarcomeric myosin is possible, but expensive and very time consuming. In collaboration with the Leinwand laboratory at the University of Colorado, Boulder, and the Spudich laboratory at Stanford University, we have begun to look at some of these mutations in human β-cardiac myosin; for example, R453C associated with hypertrophic cardiomyopathy (Bloemink et al., 2014; Sommese et al., 2013). We have defined the rate and equilibrium constants of each of the steps in the cycle as shown in Fig. 1. These measurements demonstrate that the changes are all relatively small, twofold at most, and most changes are below the level of statistical significance. The exception is the rate constant of the events associated with the myosin recovery stroke (switch 2 closure, and the hydrolysis step), which take place while the myosin is detached from actin. These events are slower by at least a factor of two. We argued that the slowing of this step (from ∼14 to ∼4 s^{-1}) would increase the average time for a myosin to hydrolyse ATP and complete the recovery stroke from 70 to 250 ms. If the heart is beating once per second, then ATP hydrolysis can keep up with the demand. But under prolonged, intense exercise, when the heart can be beating three times faster at once every 300 ms, then the ATP hydrolysis rate may become limiting. This would result in depletion of the pool of M.ADP.Pi and a build-up of M.ATP in the R453C mutant. Such a build-up of M.ATP may limit the heart performance under extreme conditions and trigger some remodelling of the heart.

In a parallel study from the Spudich laboratory (Sommese et al., 2013), it was reported that the R453C mutation caused a ∼30% decrease in the V_{max} and K_m for actin for the ATPase of the motor domain of myosin, a 30% decrease in the *in vitro* velocity and a 50% increase in the intrinsic force of the motor compared with the wild type. These results predict that the overall force of the ensemble of myosin molecules in the muscle should be higher in the R453C mutant compared with the wild type, a result confirmed by a loaded *in vitro* motility assay. If we use the detailed biochemical analysis of the steps in the cycle to map the ATPase cycle as in Fig. 4, then the data predict the reduced V_{max} and K_m values. The data do not account for the increase in force, which is most easily explained by an enhanced inhibition of ADP release by load on the cross-bridge.

Examining the location of this mutation in the myosin motor (see Fig. 5) shows it to be in a surface loop that links the long O-helix in the upper 50 kDa domain with the central β-sheet, and in fact provided a direct link between the actin and nucleotide binding sites. The arginine side chain points into the interior of the protein and makes several bonds to both the O-helix and the β-sheet. This appears to help tie the two structural components together. The surface loop, the O-helix and the β-sheet are all highly conserved regions of the myosin motor domain, and the R453 is present in every sarcomeric myosin we have examined from scallop to *Drosophila* to mammals. In contrast, R453 is not present in smooth or non-muscle myosin II, nor is it present in most other myosin families. This suggests that it may be present only in sarcomeric myosins, where large and rapid forces are produced. The link between the actin and nucleotide sites may be more pliant in non-sarcomeric myosins.

Conclusions

Here we have tried to demonstrate how studies of myosin isoforms (muscle and non-muscle) have helped us to understand how force and movement are generated by actin and myosin. By studying sarcomeric myosin isoforms and naturally occurring mutations in these myosins, we can begin to tease apart the relationship between differences in isoform sequence and the physiology of the muscle fibre in both healthy and diseased tissue.

Competing interests

The authors declare no competing or financial interests.

Funding

J.W. was supported by a subcontract of NIH R01 GM29090 to Leslie Leinwand, University of Colorado, and Z.U. was supported by British Heart Fund grant no. PG 30200. Deposited in PMC for release after 12 months.

References

Bloemink, M. J. and Geeves, M. A. (2011). Shaking the myosin family tree: biochemical kinetics defines four types of myosin motor. *Semin. Cell Dev. Biol.* **22**, 961-967.

Bloemink, M. J., Adamek, N., Reggiani, C. and Geeves, M. A. (2007). Kinetic analysis of the slow skeletal myosin MHC-1 isoform from bovine masseter muscle. *J. Mol. Biol.* **373**, 1184-1197.

Bloemink, M., Deacon, J., Langer, S., Vera, C., Combs, A., Leinwand, L. and Geeves, M. A. (2014). The hypertrophic cardiomyopathy myosin mutation R453C alters ATP-binding and hydrolysis of human cardiac β-myosin. *J. Biol. Chem.* **289**, 5158-5167.

Bottinelli, R. and Reggiani, C. (2000). Human skeletal muscle fibres: molecular and functional diversity. *Prog. Biophys. Mol. Biol.* **73**, 195-262.

Colegrave, M. and Peckham, M. (2014). Structural implications of β-cardiac myosin heavy chain mutations in human disease. *Anat. Rec.* **297**, 1670-1680.

De La Cruz, E. M. and Ostap, E. M. (2004). Relating biochemistry and function in the myosin superfamily. *Curr. Opin. Cell Biol.* **16**, 61-67.

Deacon, J. C., Bloemink, M. J., Rezavandi, H., Geeves, M. A. and Leinwand, L. A. (2012). Erratum to: identification of functional differences between recombinant human α and β cardiac myosin motors. *Cell. Mol. Life Sci.* **69**, 4239-4255.

Geeves, M. A. and Holmes, K. C. (1999). Structural mechanism of muscle contraction. *Annu. Rev. Biochem.* **68**, 687-728.

Geeves, M. A. and Holmes, K. C. (2005). The molecular mechanism of muscle contraction. *Adv. Protein Chem.* **71**, 161-193.

Golomb, E., Ma, X., Jana, S. S., Preston, Y. A., Kawamoto, S., Shoham, N. G., Goldin, E., Conti, M. A., Sellers, J. R. and Adelstein, R. S. (2003). Identification and characterization of nonmuscle myosin II-C, a new member of the myosin II family. *J. Biol. Chem.* **279**, 2800-2808.

Greenberg, M. J., Lin, T., Goldman, Y. E., Shuman, H. and Ostap, E. M. (2012). Myosin IC generates power over a range of loads via a new tension-sensing mechanism. *Proc. Natl. Acad. Sci. USA* **109**, E2433-E2440.

Greenberg, M. J., Shuman, H. and Ostap, E. M. (2014). Inherent force-dependent properties of β-cardiac myosin contribute to the force-velocity relationship of cardiac muscle. *Biophys. J.* **107**, L41-L44.

Kovács, M., Thirumurugan, K., Knight, P. J. and Sellers, J. R. (2007). Load-dependent mechanism of nonmuscle myosin 2. *Proc. Natl. Acad. Sci. USA* **104**, 9994-9999.

Krendel, M. and Mooseker, M. S. (2005). Myosins: tails (and heads) of functional diversity. *Am. Physiol. Soc.* **20**, 239-251.

Kron, S. J. and Spudich, J. A. (1986). Fluorescent actin filaments move on myosin fixed to a glass surface. *Proc. Natl. Acad. Sci. USA* **83**, 6272-6276.

Moore, J. R., Leinwand, L., Warshaw, D. M., Robbins, J., Seidman, C. and Watkins, H. (2012). Understanding cardiomyopathy phenotypes based on the functional impact of mutations in the myosin motor. *Circ. Res.* **111**, 375-385.

Odronitz, F. and Kollmar, M. (2007). Drawing the tree of eukaryotic life based on the analysis of 2,269 manually annotated myosins from 328 species. *Genome Biol.* **8**, R196.

Pellegrino, M. A., Canepari, M., Rossi, R., D'Antona, G., Reggiani, C. and Bottinelli, R. (2003). Orthologous myosin isoforms and scaling of shortening velocity with body size in mouse, rat, rabbit and human muscles. *J. Physiol.* **546**, 677-689.

Piroddi, N., Belus, A., Scellini, B., Tesi, C., Giunti, G., Cerbai, E., Mugelli, A. and Poggesi, C. (2007). Tension generation and relaxation in single myofibrils from human atrial and ventricular myocardium. *Pflügers Arch.* **454**, 63-73.

Racca, A. W., Beck, A. E., Rao, V. S., Flint, G. V., Lundy, S. D., Born, D. E., Bamshad, M. and Regnier, M. (2013). Contractility and kinetics of human fetal and human adult skeletal muscle. *J. Physiol.* **591**, 3049-3061.

Resnicow, D. I., Deacon, J. C., Warrick, H. M., Spudich, J. A. and Leinwand, L. A. (2010). Functional diversity among a family of human skeletal muscle myosin motors. *Proc. Natl. Acad. Sci. USA* **107**, 1053-1058.

Schiaffino, S. and Reggiani, C. (2011). Fiber types in mammalian skeletal muscles. *Physiol. Rev.* **91**, 1447-1531.

Sommese, R. F., Sung, J., Nag, S., Sutton, S., Deacon, J. C., Choe, E., Leinwand, L. A., Ruppel, K. and Spudich, J. A. (2013). Molecular consequences of the R453C hypertrophic cardiomyopathy mutation on human ß-cardiac myosin motor function. *Proc. Natl. Acad. Sci. USA* **110**, 12607-12612.

Srikakulam, R. and Winkelmann, D. A. (1999). Myosin II folding is mediated by a molecular chaperonin. *J. Biol. Chem.* **274**, 27265-27273.

Sweeney, H. L. and Houdusse, A. (2010). Structural and functional insights into the myosin motor mechanism. *Annu. Rev. Biophys.* **39**, 539-557.

Trybus, K. M. (2008). Myosin V from head to tail. *Cell. Mol. Life Sci.* **65**, 1378-1389.

Veigel, C., Molloy, J. E., Schmitz, S. and Kendrick-Jones, J. (2003). Load-dependent kinetics of force production by smooth muscle myosin measured with optical tweezers. *Nat. Cell Biol.* **5**, 980-986.

Veigel, C., Schmitz, S., Wang, F. and Sellers, J. R. (2005). Load-dependent kinetics of myosin-V can explain its high processivity. *Nat. Cell Biol.* **7**, 861-869.

Weiss, A. and Leinwand, L. A. (1996). The mammalian myosin heavy chain gene family. *Annu. Rev. Cell Dev. Biol.* **12**, 417-439.